Biosensors and Bioelectronics 58 (2014) 145–152

Contents lists available at ScienceDirect

Biosensors and Bioelectronics

journal homepage: www.elsevier.com/locate/bios

Simple and label-free electrochemical impedance Amelogenin gene hybridization biosensing based on reduced graphene oxide

Ali Benvidi [a,b,*], Nooshin Rajabzadeh [a], Mohammad Mazloum-Ardakani [a], Mohammad Mehdi Heidari [c], Ashok Mulchandani [b,**]

[a] Department of Chemistry, Faculty of Science, Yazd University, Yazd 89195-741, Iran
[b] Department of Chemical and Environmental Engineering, University of California, Riverside, CA 92521, USA
[c] Department of Biology, Faculty of Science, Yazd University, Yazd 89195-741, Iran

ARTICLE INFO

Article history:
Received 8 November 2013
Received in revised form
22 January 2014
Accepted 28 January 2014
Available online 28 February 2014

Keywords:
DNA biosensor
DNA hybridization
Amelogenin gene
Graphene
Electrochemical impedance spectroscopy

ABSTRACT

The increasing desire for sensitive, easy, low-cost, and label free methods for the detection of DNA sequences has become a vital matter in biomedical research. For the first time a novel label-free biosensor for sensitive detection of Amelogenin gene (AMEL) using reduced graphene oxide modified glassy carbon electrode (GCE/RGO) has been developed. In this work, detection of DNA hybridization of the target and probe DNA was investigated by electrochemical impedance spectroscopy (EIS) and cyclic voltammetry (CV). The optimum conditions were found for the immobilization of probe on RGO surface and its hybridization with the target DNA. CV and EIS carried out in an aqueous solution containing $[Fe(CN)_6]^{3-/4-}$ redox pair have been used for the biosensor characterization. The biosensor has a wide linear range from 1.0×10^{-20} to 1.0×10^{-14} M with the lower detection limit of 3.2×10^{-21} M. Moreover, the present electrochemical detection offers some unique advantages such as ultrahigh sensitivity, simplicity, and feasibility for apparatus miniaturization in analytical tests. The excellent performance of the biosensor is attributed to large surface-to-volume ratio and high conductivity of RGO, which enhances the probe absorption and promotes direct electron transfer between probe and the electrode surface. This electrochemical DNA sensor could be used for the detection of specific ssDNA sequence in real biological samples.

1. Introduction

Nucleic acid hybridization has become a fundamental technique in biology for the detection and analysis of specific DNA sequences. The detection of specific nucleic acid sequences has become increasingly important in the diagnosis and treatment of genetic disease, detection of infectious agents, drug screening, food safety, and environmental monitoring (Chen et al., 2009; Kalogianni et al., 2006). Many attempts have been made to generate inexpensive, easy-to-use, fast-response devices to address the challenges connected to the development of DNA biosensors. Electrochemical-based sensors have attracted more attention than other methods because they are highly sensitive, easy, inexpensive, and compatible with micro fabrication technologies (White and Plaxco, 2010). DNA electrochemical biosensors based on demonstrating the variations between single-stranded DNA (ss-DNA) probes and hybridized DNA (ds-DNA) have attracted great interest (Jin et al., 2007).

Graphene has been introduced as the building block of graphite for more than 60 years, but its experimental isolation was first attained in 2004. In spite of its short history, graphene has attracted much notice because of its excellent mechanical, thermal and electronic properties (Novoselov et al., 2004). This unique nanostructure holds vast promise for potential applications in many technological fields such as Nano electronics (Xinhuang, et al., 2009), biosensors (Xiao et al., 2013), Nano composites (Hu et al., 2011a, 2011b), batteries, super capacitors (Vivekchand et al., 2008), gas sensors (Leenaerts et al., 2008), pH sensor (Ang et al., 2008) and hydrogen storage (Geim and Novoselov, 2007). Graphene is composed of planar sheets of sp^2 bonded carbon atoms. The most common approach to graphite exfoliation is the use of a strong oxidant for obtaining graphene oxide (GO) as nonconductive hydrophilic carbon material. As recently proved, the solution-based route involves chemical oxidation of graphite to hydrophilic graphite oxide, which can be readily exfoliated as GO sheets by ultra-sonication in water. Graphene oxide can be reverted back to conducting graphene by chemical reduction, for example, using hydrazine (Stankovich et al., 2006). This unique nanostructure

* Corresponding author at: Department of Chemistry, Faculty of Science, Yazd University, Yazd 89195-741, Iran. Tel.: +98 351 8122645; fax: +98 351 8210644.
** Corresponding author. Tel.: +1 952 827 6419.
E-mail addresses: abenvidi@yazduni.ac.ir, benvidi89@gmail.com (A. Benvidi), adani@engr.ucr.edu (A. Mulchandani).

http://dx.doi.org/10.1016/j.bios.2014.01.053
0956-5663

material has high surface area, excellent electrical conductivity and electron mobility at room temperature, robust mechanical properties, and flexibility. These special properties of graphene may provide to fabricate novel biosensors for virtual applications. The high surface area is helpful in increasing the surface loading of the probe DNA. The excellent conductivity and small band gap are favorable for conducting electrons from the biomolecules (Stankovich et al., 2006). Graphene-based chemical sensors can also have a much higher sensitivity because of the low electronic noise from thermal effect (Ao et al., 2008; Pozo et al., 2005). Furthermore, compared with CNTs, graphene can be obtained easily by chemical change of the inexpensive graphite (Xu et al., 2008).

Sex determination using genomic DNA from several origins is often an important tool in forensic science or in routine genotyping. AMEL is one of the major matrix proteins secreted by the tooth enamel (Faerman et al., 1995). The AMEL gene, coding for a highly conserved protein, is located on the X and the Y chromosomes in humans. The two alleles are similar for the exonic sequences but differ in the intronic sequences (Slavkin, 1997). Thus the females (XX) have two identical AMEL genes but the males (XY) have two non-identical genes. AMEL is a very useful marker for sex determination especially in forensic applications, where the determination of gender in biological samples has a primary importance for evidentiary and investigative purposes.

EIS has increasingly become method of choice for electrochemical measurements of molecular interactions and is widely used in a variety of biosensing applications (Lisdat and Schafer, 2008). There are a growing number of publications on the use of EIS based on immobilized DNA probes, to detect complementary ssDNA target through hybridization. The method is very sensitive and can be used for detection of a wide range of molecular recognition events happening on the electrode surface without any label. The method provides unique advantages compared to other electrochemical methods, such as high sensitivity and ability to separate the surface binding events from the solution impedance. EIS is a method of measuring the impedance value of the electrode surface during the process of frequency variation. EIS is able to provide various properties of interface of the electrode and solution, including the electrode impedance, capacitance of the electric double layer, and the surface electron transfer resistance (R_{ct}). This technique can be used to characterize a DNA hybridization sensor to realize sensitive indicator-free detection of the gene sequences. Hybridization reaction of DNA on the electrode surface results in change of the R_{ct} value upon formation of duplex between probe and target DNA. The quantity of the negative charge on the electrode surface increases greatly due to DNA duplex formation and thereby further impeding the electron transfer.

In this article, we report a new, simple, ultra-sensitive, highly selective and label-free electrochemical AMEL gene hybridization biosensor based on reduced graphene oxide as the platform. All the processes including modification of GCE with RGO, ss-DNA immobilization and complementary sequence hybridization were studied using both CV and EIS techniques. DNA immobilization, hybridization on the platform caused changes in the interfacial and conformation, which could be readily monitored by impedance measurement. Under optimal conditions the device can achieve high sensitivity to detect 3.2×10^{-21} M and high selectivity in real samples of target DNA. Because of this extremely low detection limit we believe that our explorations may present a basis for further research and advancement in graphene-based impedimetric biosensing. These results confirm that the AMEL gene can be used for rapid sex determination with a high efficiency and accuracy. In our previous paper, carbon paste electrode (CPE) was modified with gold nanoparticles (AuNPs) for immobilization of thiolated bioreceptors (Mazloum-Ardakani et al., 2013). Although elegant it had disadvantages of (1) low reproducibility due to use of carbon paste electrode; (2) long assay time because of the time required for hybridization reactions and self-assembly of ssDNA in the presence of methylene blue; and (3) high detection limit. To eliminate of these disadvantages, we propose to the best of our knowledge for the first time the determination of AMEL gene by label-free electrochemical impedance method on reduced graphene oxide modified GCE. The newly developed sensor had an extremely high sensitivity, a low limit of detection, a wide dynamic range, an excellent selectivity and a short assay time. The biosensor successfully detected the AMEL gene in real samples.

2. Experimental

2.1. Materials

Specific primers and probes were designed based on AMEL gene obtained from the Gen Bank database. The oligonucleotides were designed by primer design software (Premier 5.0, Premier Biosoft, Canada), and their secondary structure were examined with Gene Runner (version 3.05, Hastings Software, USA). Deoxyribonucleotide triphosphate (dNTP) and Taq DNA polymerase were purchased from Sina Clon Company, Iran. All oligonucleotides were synthesized by Macrogen (Korea). Chemical reagents including absolute ethanol, sodium dihydrogen phosphate, disodium hydrogen phosphate, 1-ethyl-3-(3-dimethyl amino propyl) carbo-diimide hydrochloride (EDC), N-hydroxysuccinimide (NHS), 2-(N-morpholino) ethane sulfonic acid (MES), Tween 20 (Polyoxyethylenesorbitan monolaurate), potassium ferrocyanide, potassium ferricyanide, graphite powders, $KMnO_4$, hydrazine monohydrate (N_2H_4, 98%) and sulfuric acid were purchased from commercial sources (Merck or Sigma) in analytical grade and used without further purification. All solutions were prepared with deionized water (DI: 18 MΩ cm^{-1} resistivity).

The sequences are as follows:

Probe sequence:
AMGX: 3′-TATCCCAGATGTTTCTC-NH_2-5′
Complementary sequence:
AMGX: 3′-GAGAAACATCTGGGATA-5′
Noncomplementary sequence (random sequence):
AMGY: 5′-CACTTTATTTGGGATG-3′

The stock solutions of the oligonucleotides (100.0 μM) were prepared in 0.1 M pH 7.4 phosphate buffer saline (PBS) and kept frozen at −20 °C. The washing solution was 0.05 M phosphate buffer (pH=7.4) containing 0.3 M of NaCl. The pH was adjusted with either NaOH or HCl solutions. The double distilled water and buffers were sterilized using autoclave.

2.2. Instrumentation

The electrochemical measurements were performed with an Autolab potentiostat/galvanostat model PGSTAT 30 (Eco Chemic, Utrecht, Netherlands) and a NOVA 1.7 software at laboratory temperature (25 ± 1 °C). The utilized three-electrode system was composed of a glassy carbon working electrode (surface area of 7.07 mm^2), an Ag/AgCl (1.0 M KCl) reference electrode, and a platinum auxiliary electrode. All the potentials in the text are reported with respect to the reference electrode. The pH measurements were done with a Metrohm model 691 pH/mV meters. CV was recorded at a scan rate of 100 mV s^{-1} and EIS measurements were recorded between 100 kHz and 0.01 Hz at 10 mV, AC amplitude. All experiments were carried out in 0.5 mM [Fe

$(CN)_6]^{3-/4-}$ (1:1 M ratio) as a redox probe in 0.1 M PBS solution in the Faraday cage. The impedance spectra obtained were represented as Nyquist plots and fitted by a Randles equivalent circuit.

UV–vis spectra of GO and GR were acquired with a spectrophotometer Optizen model 3220 from 400 to 900 nm using a glass cuvette with 1 cm path length. The infrared spectra of GO and RGO were done with Equinox instrument model 55 Bruker. Scanning electron microscopy (SEM) was performed with TESCAN instrument model VEGA3 and X-ray photoelectron spectroscopy (XPS) characterization was carried out by XPS 8025-BesTec (Germany) with Al Ka X-ray source ($h\nu = 1486$ eV) at a vacuum $< 10^{-7}$ Pa. The XPS peaks were deconvoluted by Gaussian/Lorentzian component after background subtraction.

2.3. Synthesis of reduced graphene oxide (RGO)

GO was obtained by oxidizing graphite using an improved method (Marcano et al., 2010). Briefly, a mixture of concentrated H_2SO_4/H_3PO_4 (360:40 mL) was added to a mixture of graphite/$KMnO_4$ (3:18 g) at 50 °C and stirred for 12 h. The reaction mixture was cooled to room temperature and transferred onto ice with 30% H_2O_2 (3 mL). The obtained solution was centrifuged, and then filtered. The solid material was then washed with water, 30% HCl, and finally washed twice with 200 mL of ethanol. A colloidal suspension of graphene oxide in purified water (150 mg/50 mL) was prepared by sonication for 3 h. The suspension of RGO was subsequently added to 50 μL of hydrazine solution (98%) with 200 μL of ammonia solution (30% in water), refluxed at 90 °C for 12 h and cooled to room temperature. Subsequently, the solution was centrifuged, and the RGO pellet washed with deionized water and then dried at 60 °C in vacuum for 24 h. This process for the preparation RGO was performed three times and the best RGO was used for the modification of the electrode surface.

2.4. Preparation of probe-modified electrode

Scheme 1 illustrates of the schematic of electrochemical biosensor fabrication. The process started with polishing of the glassy carbon electrode using 0.05 μm alumina slurry, rinsing with DI water followed by sonication for 30 min each in ethanol and water. The GCE was then modified by dropping 100 μL 0.05 g mL^{-1} suspension of RGO on the electrode surface held upside-down, covering with a plastic cap and drying overnight at room temperature (GCE/RGO).

To immobilize the DNA probes on the electrode, carboxylic acid groups of RGO were activated by immersing the electrode in a solution containing 0.2 M EDC in MES buffer and 0.5 M NHS for 1 h and washed with 0.1 M PBS. Eighty μL of 1 μM of the 5′-amino terminated DNA probes solution was dispensed on the surface of resulting electrode held upside-down and kept for 1 h at 25 °C while covered with a glassy cap to protect the solution from evaporation (GCE/RGO/AMEL). Prior to use, the modified electrode was rinsed with 0.1 M PBS buffer and incubated with 0.1% Tween 20 solution for 75 min to both displace nonspecifically bound/adsorbed oligonucleotides and prevent nonspecific binding of oligonucleotides during analysis/detection of samples. Finally the functionalized electrode was rinsed with DI water and incubated in 0.1 M PBS buffer solution (pH = 7.4) prior to use. Each step of modification was followed using CV and EIS.

2.5. Genomic DNA extraction

DNA was isolated from peripheral blood samples using a DNA extraction kit (DNA fast Kit-Gen fanavaran, Tehran, Iran). Polymerase chain reaction (PCR) amplification of genomic DNA was performed using one pairs of primers (5′-CCCTGGGCTCTGTAAAGAATAGTG-3′ and 5′-ATCAGAGCTTAAACTGGGAAGCTG-3′) of Amelogenin gene. PCR amplification was performed in a final volume of 25 μL containing 100 ng total DNA as a template, 0.5 μL each primers (10 pmol), 0.8 μL $MgCl_2$ (50 mM), 0.5 μL of dNTP (10 mM), 2.5 μL of 10X PCR buffer and 1.5 Units Taq DNA polymerase. The PCR was performed based on the following conditions: initial denaturation at 94 °C for 5 min; followed by 35 cycles including denaturation at 94 °C for 35 s, annealing at 62 °C for 35 s, and extension at 72 °C for 90 s; and a final extension at 72 °C for 5 min. The PCR product was diluted and the concentration was determined by measuring the absorbance by a UV–vis spectrophotometer (Sauners, 1999). The concentration of diluted PCR product was 0.01 ng/mL. The PCR products were electrophoresed on 1.5% agarose gel and stained with ethidium bromide.

3. Results and discussion

3.1. Characterization of graphene oxide and reduced graphene oxide

Fig. S1 shows UV/vis absorption spectra of GO before and after hydrazine reduction; the two spectra were recorded for an equal concentration of each material. UV/vis spectrum of GO shows strong absorption band attributed to $\pi \rightarrow \pi^*$ transitions of aromatic

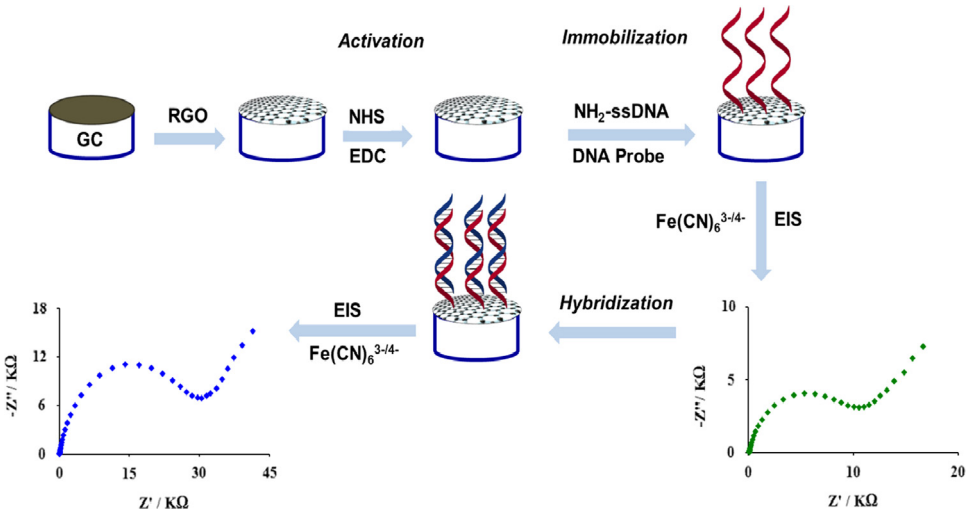

Scheme 1. Illustration of the experimental procedure for electrochemical DNA sensing.

C = C bonds (Hu et al., 2012). The UV/vis spectra of this material suggest that the more ordered structure of GO is due to greater retention of carbon rings in the basal planes. The degree of remaining conjugation can be determined by the λ_{max} of each UV/vis spectrum. The more $\pi \rightarrow \pi^*$ transitions (conjugation), the less energy needs to be used for the electronic transition, which results in a higher λ_{max} (Marcano et al., 2010). The prepared GO displays two characteristics bands: a strong absorption band with a maximum at 228 nm and a shoulder at around 300 nm. Reduction of GO resulted in a red shift of the main absorption band to 273 nm. In addition, the intensity of the absorption tail in the higher λ was significantly increased (Fig. S1), suggesting that the GO nanosheets have been reduced and the electronic conjugation within the GO nanosheet was restored upon hydrazine reduction (Wang et al., 2013).

Fig. S2 shows the infrared spectra of GO and RGO. The IR spectrum of GO shows a C – O stretch at 1222 cm^{-1} and O – H stretch at 3500–3300 cm^{-1} as well as a C = O stretch at 1720–1690 cm^{-1} (Lomeda et al., 2008). On the other hand, IR of RGO shows absence of the peaks at 1720–1690 and 1222 cm^{-1}, indicating removal of the epoxide and carboxyl groups attached to the basal graphene layer. As the results show, while the hydrazine treatment reduced the oxygenated groups in GO restoring a large fraction of the electrical conductivity, it did not remove them completely. There were enough carboxylic acid groups remaining in the RGO for grafting the DNA probes to the graphene surface by carbodiimide chemistry.

Fig. S3 shows scanning electron microscopy (SEM) image of the RGO prepared in this work. The image show a highly porous structure with a large surface area made of petal-like graphene nanoflakes with large lateral sizes and sharp edges in random directions oriented preferentially vertically to the substrate. This morphology of the RGO is expected to provide unique electrochemical properties with high activity due to the formation of a large fraction of graphitic edge-plane defects combined with a large surface area.

Fig. S4 shows the X-ray photoelectron spectra (XPS) of RGO and deconvoluted C1s peak (Fig. S4, inset) after application of mixed Gaussian/Lorentzian functions to fit the C1s peak of XPS data. The exhibited peaks centered at ~284.5 eV, ~285.5 eV, ~286.5, ~288.5 eV and ~289.3 eV are attributed to sp^2-hybridized carbon atoms (C=C), carbon in aldehyde group (C–O), ether/epoxy group (C–O–C), carbonyl group (C=O) and carboxylic carbon (O–C=O), respectively (Campos-Delgado et al., 2009,2008). A calculation of the area percent of the RGO functional groups (Table S1), revealed the RGO to still contain a significant amount of COOH groups allowing for a facile route of covalently grafting NH_2-DNA probe using a zero-length linker.

3.2. Electrochemical characterization of the modified electrode

Fig. 1 shows the CVs of 0.5 mM ferrocyanide ion on bare GCE, GCE/RGO, and GCE/RGO/AMEL electrodes and GCE/RGO/AMEL after hybridization with different concentrations of complementary target DNA. As shown in the figure, the peak current (i_p) of GCE/RGO electrode was significantly higher when compared to unmodified GCE which is attributed to the increased surface area and excellent conductivity of RGO (Stankovich et al., 2006). Upon functionalizing the GCE/RGO electrode with the probe DNA for AMEL gene the peak current decreased and the peak potential separations (ΔE_p) increased significantly. These changes are attributed to (1) blocking of the electrode surface by DNA and the repulsion of negatively charged redox probes ($[Fe(CN)_6]^{3-/4}$) from the electrode by the negative charge of the DNA phosphate backbone (Kashefi-Kheyrabadi and Mehrgardi, 2012). Following hybridization of the DNA probe with the complementary DNA, there was a further increase of ΔE_p and decrease of peak redox currents which are ascribed to the more electrode surface blocking because of hybridization and increased repulsion between negatively charged DNA hybrids and $[Fe(CN)_6]^{3/4-}$ anions.

The typical Nyquist plot includes a semicircle, at a higher frequency corresponding to the electron transfer limited process, with its diameter equal to the electron transfer resistance (R_{ct}), and a linear part at a lower frequency representing the diffusion-limited process. The EIS technique was used to monitor RGO modification of GCE, immobilization of probe DNA and hybridization of probe with complementary target sequences by observing the charge transfer process of the redox probe $[Fe(CN)_6]^{3-/4-}$ on the electrode surface. Fig. 2 shows the Nyquist plots of the

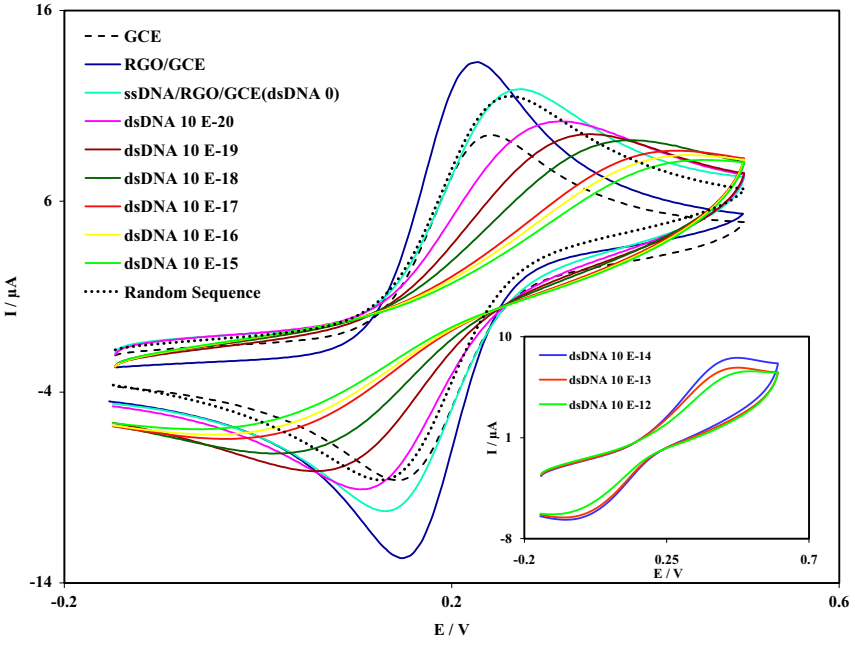

Fig. 1. Cyclic voltammograms in 0.5 mM $[Fe(CN)_6]^{3-/4-}$ in 0.1M KCl for bare GCE, GCE/RGO, ssDNA/GCE/RGO, and after hybridization with different concentration of its complementary DNA.

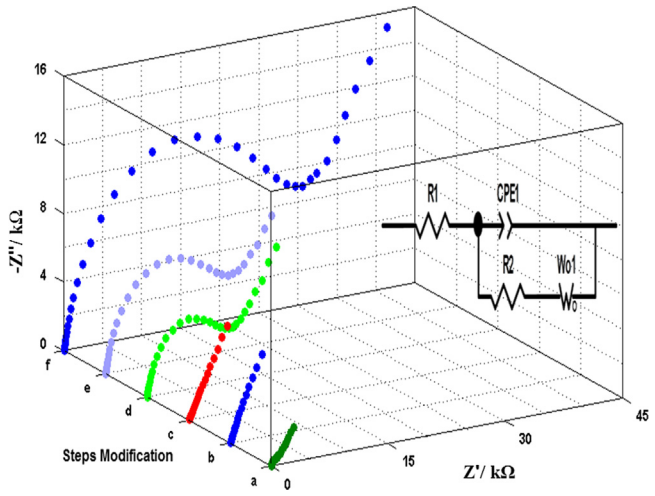

Fig. 2. Nyquist plots for (a) bare GCE, (b) GCE/RGO, (c) activated carboxylic groups using EDC/NHS, (d) after capture immobilization, (e) after incubation of Tween solution and (f) after hybridization with target with concentration 1.0×10^{-16} M. EIS measurements were performed in $[Fe(CN)_6]^{3-/4-}$ (0.5×10^{-3} M; 1:1) as a redox probe, at a constant DC potential of +0.2V. Inset: equivalent circuit used to model impedance data in the presence of redox couples; R_1, electrolyte solution resistance; R_2, interfacial electron transfer resistance; CPE_1, constant phase element; W_{01}, Warburg impedance resulting from the diffusion of ions.

electrode after each modification step. The Randles equivalent circuit, shown in Fig. 2 inset, was used to analyze the Nyquist plots after each surface modification steps in biosensor fabrication and sensing of target DNA. In this equivalent circuit, R_1 is the electrolyte resistance (0.5 mM $[Fe(CN)_6]^{3-/4-}$ and 0.1 M KCl) and was between 120 and 130 Ω; $W_{01,}$ is Warburg impedance resulting from the diffusion of ions and ranged from 160–180 $\mu\Omega^{-1}$; CPE is constant phase element and was in the range of 0.781–9.6 $\mu F\,cm^{-2}$; and R_2/R_{ct} is the electron transfer resistance which changed after each step of electrode modification and sensing. The values of R_1, W_{01} and CPE were in agreement with the literature (Park et al., 2008). Among these electrical parameters, we focused on the R_{ct} value recorded after each modification step, since electron transfer process of $[Fe(CN)_6]^{3-/4-}$ was strongly influenced by electrode modification. In Nyquist diagram, the R_{ct} could be directly related to the semicircle diameter. The results show that the R_{ct} of GCE decreased when RGO were immobilized on the GCE surface indicating an easy electronic transport at the electrode surface upon modification with RGO. The subsequent modification of the GCE/RGO surface with the probe DNA, treatment with Tween 20 and hybridization of DNA probe with complementary DNA increased the R_{ct} values after each step. These increases may be ascribed to increase in the double layer capacitance resulting from the electrostatic repulsion of negatively charged $[Fe(CN)_6]^{3-/4-}$ redox probe due to accumulation of negative charges resulting from DNA probe, surfactant Tween 20 and complementary DNA. This is in accordance with the results of CV where the increased repulsion of redox probe by the increasing negative charge at the electrode surface resulted in lower peak currents and increased peak potential separation. The double-layer capacitance of the final electrode, i.e. after functionalizing with RGO, attachment of ssDNA probe, Tween 20 blocking and hybridization with 10^{-20} M, the lowest concentration, of complementary DNA at 25 °C was 30.8 $\mu F\,cm^{-2}\pm0.5$ ($n=3$). This value will increase with increase of complementary DNA concentration.

3.3. Optimization of operating conditions

For increasing the sensitivity and selectivity of DNA biosensor, experimental conditions including immobilization time of probe DNA, hybridization time and temperature and Tween modification time were optimized. The change in specific electron charge transfer resistance ($\Delta R_{ct}=(R_{ct})_{final}-(R_{ct})_{initial}$) was adopted as the measurement signal.

In DNA hybridization biosensors, the amount of DNA probe immobilized on the electrode is important. Increasing the amount of probe oligonucleotides would markedly upgrade the detection ability of DNA biosensor. In order to increase the amount of immobilized DNA probe and improve its DNA hybridization efficiency the effect of the ssDNA immobilization time on the RGO modified GCE was investigated. The results of this investigation are reported in Fig. 3A. The change in specific electron charge transfer resistance ($\Delta R_{ct}=(R_{ct})_{after\ immobilization}-(Rct)_{before\ immobilization}$) was adopted as the measurement signal. As the results show, ΔR_{ct} value increased with the increase of the probe immobilization time up to about 60 min and then plateaued. This may be due to the full coverage of the electrode surface by the DNA probe after 60 min. A probe immobilization time of 60 min therefore was selected in subsequent studies.

For the removal of nonspecifically adsorbed probe molecules from the electrode surface, the modified electrode was incubated in the solution of Tween surfactant (0.1% v/v) for a determined time. Tween solution not only removes these DNA molecules from the electrode surface, but also can fill the pinholes among DNA monolayer thereby blocking non-specific binding during analysis (Berggren et al., 1999). The EIS results (Fig. 3B) revealed that ΔR_{ct} value increased with prolongation of incubation time up to about 75 min and then leveled off. Based on these results, an incubation period of 75 min with 0.1% Tween solution was selected for future work.

Having optimized the electrode preparation factors, the effect of hybridization time and temperature on were investigated. Hybridization time was changed from 3 to 20 min while keeping hybridization temperature and complementary target DNA concentration constant at 25 °C and 1 pM, respectively. As shown in Fig. 3C, 10 min was the optimum hybridization time and was used in subsequent experiments.

Fig. 3D shows the effect of hybridization temperature on ΔR_{ct} value for hybridization with 1 pM target complementary DNA for 10 min. Results revealed that the ΔR_{ct} value initially increased reaching a maximum at around 41.5 °C and then rapidly decreased when the temperature was increased. Higher temperature leads to uncoiling of the probe and target strands and making them more accessible to each other and thereby improved efficiency of hybridization. However, the hybridization efficiency decreases when the temperature was higher than the melting temperature (48 °C) of the probe-target hybrid. Therefore, temperature of 41.5 °C was chosen as optimum hybridization temperature.

3.4. Analytical characterization

Fig. 4 shows the EIS response of the GCE/RGO/AMEL biosensor to the addition of different concentrations of complementary target DNA. As expected the R_{ct} values increased with increasing concentration of complementary target DNA as a result of increased negative charge of duplex DNA which impedes the access of $[Fe(CN)_6]^{3-/4-}$ redox probe to the electrode surface. Fig. 4 inset shows the plot for relationship between ΔR_{ct} value and log of target DNA concentration, calibration plot, where in the response for a sample solution with no target DNA was considered as initial/control R_{ct}. Each data point in the calibration plot (Fig. 4) is the mean of measurements from 3 independent biosensors prepared and used on the same day. The results show the calibration plot is constituted of two linear segments, first from 1.0×10^{-20} to 1.0×10^{-14} M and second from 1.0×10^{-14} to 1.0×10^{-10} M. that are represented by linear regression equations

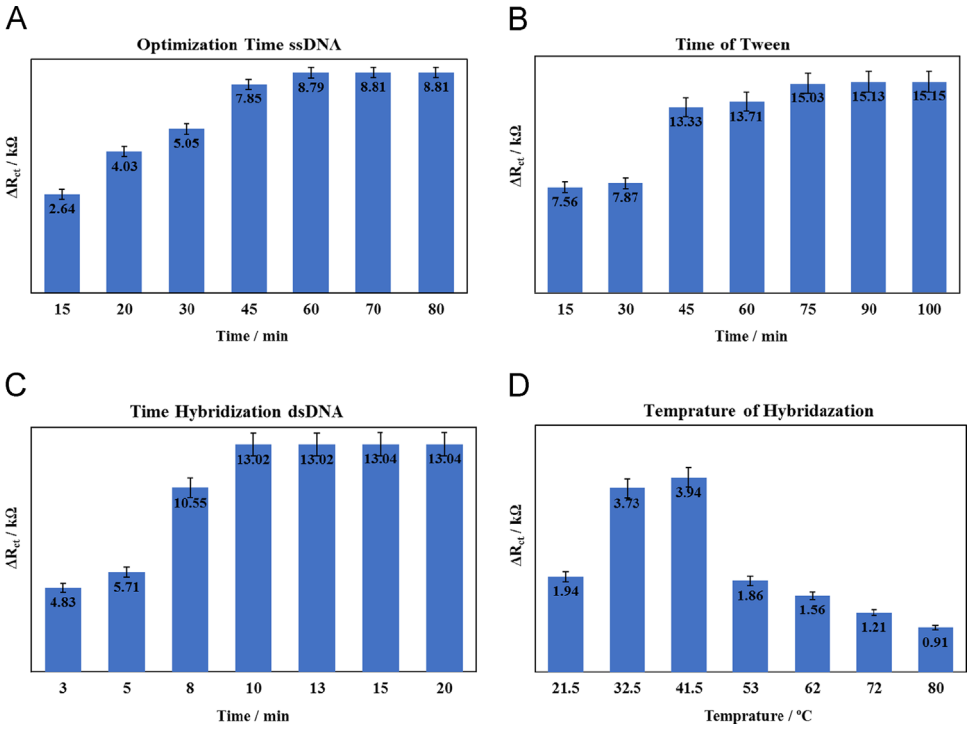

Fig. 3. Optimization of operating conditions: (A) effect of time of DNA probe immobilization, (B) effect of time of hybridization with target DNA, (C) effect of hybridization temperature and (D) effect of time of Tween treatment. The error bars correspond to the ± 1 standard deviation.

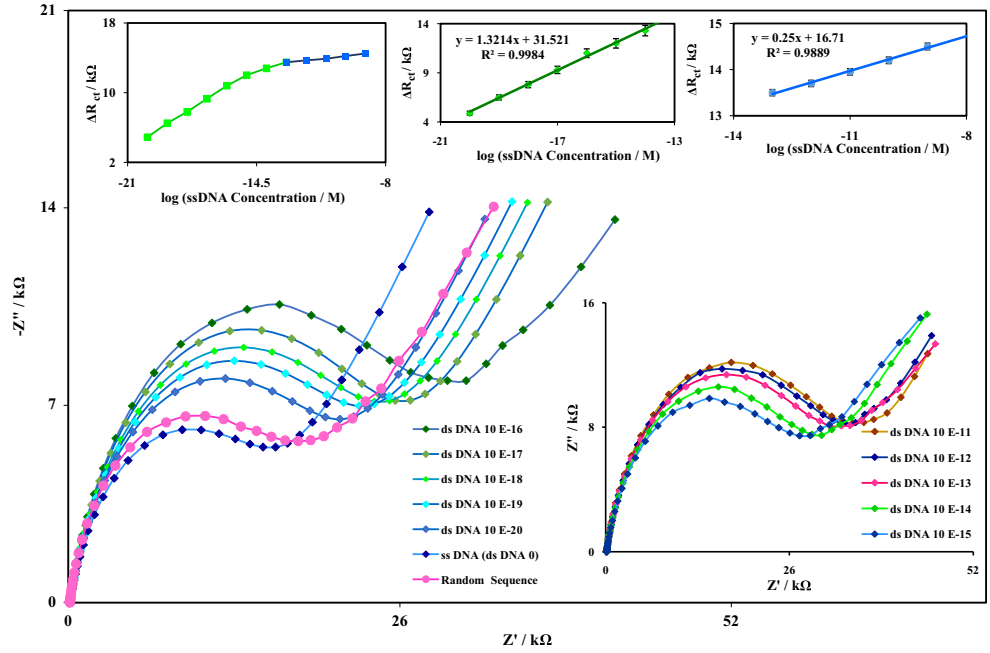

Fig. 4. Nyquist plots of the GCE/RGO/AMEL electrode before and after hybridization with different concentration of complementary DNA. Inset plots show the dependence of ΔR_{ct} on the concentration of target. Each point is the mean of measurements from 3 independent biosensors, and the error bars correspond to the ± 1 standard deviation.

ΔR_{ct} (kΩ) = 1.3214 log C (M) + 31.521 and having a regression correlation coefficient of 0.9934 and ΔR_{ct} (kΩ) = 0.25 log C (M) + 16.71 having linear regression correlation coefficient of 0.9889, respectively. The lower detection limit, C_m, was estimated to be 3.2×10^{-21} M with $3s_{bl}$ (s_{bl} was the relative standard deviation of 15 replicate measurements of the blank solution). The result indicated that the label-free electrochemical strategy based on functionalized reduced graphene oxide exhibited high sensitivity. These analytical characteristics are significantly superior to other DNA biosensors reported in the literature (Table 1). The improved performance for our platform is attributed to the uniform, well-defined structure of DNA immobilized on RGO keeping the natural characteristics of DNA in hybridized states.

A real world application requires that a sensor should be able to differentiate the target DNA from others, in this case differentiate between the perfectly complimentary DNA sequence AMGX from the non-complimentary DNA sequence AMGY. To evaluate the specificity, the response of GCE/RGO/AMEL biosensor to DNA

Table 1
Comparison of the proposed platform with others for specific DNA sequence hybridization detection.

Electrode	Modifier	Dynamic range (M)	Limit of detection (M)	Reference
ITO	Graphene–silica–gold	1.0×10^{-14}–1.0×10^{-10}	1.0×10^{-15}	Du et al., 2011
GCE	Graphene–PTCA[1]	1.0×10^{-6}–1.0×10^{-12}	5.0×10^{-13}	Hu et al., 2011
GCE	Graphene–nanostructure gold	5.0×10^{-12}–5.0×10^{-14}	3.4×10^{-15}	Liu et al., 2013
GCE	graphene oxide	1.0×10^{-6}–1.0×10^{-12}	1.1×10^{-13}	Hu et al., 2012
GCE	graphene oxide	1.0×10^{-8}–1.0×10^{-15}	2.5×10^{-16}	Yang et al., 2013
GCE	Reduce graphene Nanosheet	1.0×10^{-2}–2.0×10^{-11}	5.4×10^{-21}	Akhavan et al., 2012
GCE	Reduced graphene oxide	1.0×10^{-20}–1.0×10^{-14}	3.2×10^{-21}	This work

[1] 3, 4, 9, 10-perylene tetracarboxylic acid.

sequence AMGY extracted from blood using DNA extraction kit was evaluated. As shown in Table S2, the non-complimentary DNA AMGY generated an insignificant change in charge transfer resistance values (ΔR_{ct}) for the biosensor after incubation with AMGY for 10 min. This confirmed the ability of the bioprobe to differentiate AMGX from AMGY.

3.5. Reproducibility, stability and detection of real sample

The reproducibility of any biosensing platform is very important in DNA hybridization detection. To investigate the reproducibility, three independent GC/RGO/AMEL biosensors were prepared on the same day using the same batch of RGO and ssDNA probe and their response to 1.0×10^{-16} M of target DNA was measured. ΔR_{ct} values determined from Nyquist plots before and after hybridization were calculated to be 10.1, 9.8, 10.8 kΩ respectively. A relative standard deviation (RSD) of 5.014% for the ΔR_{ct} values of three independently made electrodes demonstrated a high reproducibility of the newly developed DNA hybridization detection platform.

The stability of ssDNA on the platform surface plays a critical role in obtaining good sensitivity. To investigate the stability of the ssDNA on the platform, the electrode was incubated in 0.1 M PBS buffer solution at 25 °C for three day. Then the GCE/RGO/AMEL was tested in 0.5 mM $[Fe(CN)_6]^{3-/4}$ (1:1 M ratio) solution by EIS according to the procedure. The results showed that the incubated electrode had almost the same behavior as freshly prepared electrode (data not shown).

The biosensor was applied to analyze the AMEL gene in real blood samples. Three distinct samples of DNA were extracted from the blood of a single person using a DNA extraction kit and amplified using PCR. The PCR amplified product was denatured by heating to 90 °C for 3 min, hybridized with the probe DNA immobilized on GCE/RGO and analyzed by EIS. For the background/control measurement, PCR was performed without the DNA sample, heated to 90 °C for 3 min to denature, hybridized with probe DNA immobilized on GCE/RGO and analyzed by EIS. A change in charge transfer resistance ($\Delta R_{ct}=(R_{ct})_{\text{after hybridization}}-(R_{ct})_{\text{before hybridization}}$) of 13.60 ± 0.05 kΩ ($n=3$) was measured. In comparison a ΔR_{ct} of 0.1 kΩ was measured for the control (no DNA). This significant increase in the ΔR_{ct} value between the electrode hybridized with PCR amplified product containing the extracted DNA compared to that with the PCR product containing no DNA (control) confirmed that this electrochemical DNA biosensor could effectively detect the PCR product of AMEL gene in real samples.

4. Conclusions

We have developed an extremely sensitive label-free electrochemical biosensor for DNA detection. The biosensor was based on glassy carbon electrode modified with RGO on which DNA probe was covalently immobilized. The RGO used had high porosity with a large surface area consisting of petal-like graphene nanoflakes with large lateral sizes oriented preferentially vertically to the substrate and contributed to high electrochemical activity. Operating at the optimum conditions, the biosensor exhibited a wide dynamic range (1.0×10^{-20} M to 1.0×10^{-14} M) and detected as low as 3.2×10^{-21} M complimentary DNA. The biosensor was applied for detection of Amelogenin gene (AMEL) in blood after extraction and amplification. We envision that this technique holds great potential for improving medical diagnosis and treatments, and could be extended to detect a large range of other targets at low concentrations.

Acknowledgments

The authors wish to thank the Yazd University Research Council, IUT Research Council and Excellence in Sensors for financial support of this research.

Appendix A. Supplementary material

Supplementary data associated with this article can be found in the online version at http://dx.doi.org/10.1016/j.bios.2014.01.053.

References

Akhavan, O., Ghaderi, E., Rahighi, R., 2012. ACS Nano 6, 2904–2916.
Ang, P.K., Chen, W., Wee, A.T.S., Loh, K.P., 2008. J. Am. Chem. Soc. 130, 14392–14393.
Ao, Z.M., Yang, J., Li, S., Jiang, Q., 2008. Chem. Phys. Lett. 461, 276–279.
Berggren, C., Stalhandske, P., Brundell, J., Johansson, G., 1999. Electroanalysis 11, 156–160.
Chen, H., Liu, X.J., Liu, Y.L., Jiang, J.H., Shen, G.L., Yu, R.Q., 2009. Biosens. Bioelectron. 24, 1955–1961.
Campos-Delgado, J., Farhat, H., Kim, Y.A., Reina, A., Kong, J., Endo, M., Muramatsu, H., Hayashi, T., Terrones, H., Terrones, M., Dresselhaus, M.S., 2009. Small 5, 2698–2702.
Campos-Delgado, J., Romo-Herrera, J.M., Jia, X.T., Cullen, D.A., Muramatsu, H., Kim, Y.A., Hayashi, T., Ren, Z.F., Smith, D.J., Okuno, Y., Ohba, T., Kanoh, H., Kaneko, K., Endo, M., Terrones, H., Dresselhaus, M.S., Terrones, M., 2008. Nano Lett. 8, 2773–2778.
Du, Y., Guo, S., Dong, S., Wang, E., 2011. Biomaterials 32, 8584–8592.
Faerman, M., Filon, D., Gila, K., Greenblatt, C.L., Smith, P., Oppenheim, A., 1995. Gene 167, 327–332.
Geim, A.K., Novoselov, K.S., 2007. Nat. Mater. 6, 183–191.
Hu, Y., Li, F., Han, D., Wu, T., Zhang, Q., Niu, L., Bao, Y., 2012. Anal. Chim. Acta 753, 82–89.
Hu, Y., Li, F., Bai, X., Li, D., Hu, S., Wang, K., Niu, L., 2011a. Chem. Commun. 47, 1743–1745.
Hu, Y., Hua, S., Li, F., Jiang, Y., Bai, X., Li, D., Niu, L., 2011b. Biosens. Bioelectron. 26, 4355–4361.
Jin, Y., Yao, X., Liu, Q., Li, J., 2007. Biosens. Bioelectron. 22, 1126–1130.
Kashefi-Kheyrabadi, L., Mehrgardi, M., 2012. Biosens. Bioelectron. 33, 184–189.
Kalogianni, D.P., Koraki, T., Christopoulos, T.K., Ioannou, P.C., 2006. Biosens. Bioelectron. 21, 1069–1076.
Leenaerts, O., Partoens, B., Peeters, F.M., 2008. Phys. Rev. B 77, 125416–125421.
Lisdat, F., Schafer, D., 2008. Anal. Bioanal. Chem. 391, 1555–1567.
Liu, A.L., Zhong, G.X., Chen, J.Y., Weng, S.H., Huang, H.N., Chen, W., Lin, L.Q., Lei, Y., Fu, F.H., Sun, Z.L., Lin, X.H., Lin, J.H., Yang, S.Y., 2013. Anal. Chim. Acta 767, 50–58.
Lomeda, J.R., Doyle, C.D., Kosynkin, D.V., Hwang, W., Tour, J.M., 2008. J. Am. Chem. Soc. 130, 16201–16209.

Marcano, D.C., Kosynkin, D.V., Berlin, J.M., Sinitskii, A., Sun, Z., Slesarev, A., Alemany, L.B., Lu, W., Tour, M., 2010. ACS Nano 4, 4806–4814.
Mazloum-Ardakani, M., Rajabzadeh, N., Benvidi, A., Heidari, M.M., 2013. Anal. Biochem. 443, 132–138.
Novoselov, K.S., Geim, A.K., Morozov, S.V., Jiang, D., Zhang, Y., Dubonos, S.V., Grigorieva, I.V., Firsov, A.A., 2004. Science 306, 666–669.
Park, J.Y., Kwon, S.H., Park, J.W., Park, S.-M., 2008. Anal. Chim. Acta 619 (1), 37–42.
Pozo, M.V.D., Alonso, C., Pariente, F., Lorenzo, E., 2005. Biosens. Bioelectron. 20, 1549–1558.
Sauners, G.C., 1999. Anal. Mol. Biol. Qual. Valid. 8, 337–376.
Slavkin, H.C., 1997. J. Am. Dent. Assoc. 128, 1021–1025.
Stankovich, S., Dmitriy, A.D., Richard, D.P., Kevin, A.K., Alfred, K., Yuanyuan, J., Yue, W., Dikin, D.A., Dommett, G.H.B., Kohlhaas, K.M., Zimney, E.J., Stach, E.A., Piner, R.D., Nguyen, S.T., Ruoff, R.S., 2006. Nature 442, 282–286.
Vivekchand, S.R.C., Rout, C.S., Subrahmanyam, K.S., Govindaraj, A., Rao, C.N.R.J., 2008. J. Chem. Sci. 120, 9–13.
Wang, Q., Das, M.R., Li, M., Boukherroub, R., Szunerits, S., 2013. Bioelectrochemistry 93, 15–22.
White, R.J., Plaxco, K.W., 2010. Anal. Chem. 82, 73–76.
Xiao, F., Li, Y., Gao, H., Ge, S., Duan, H., 2013. Biosens. Bioelectron. 41, 417–423.
Xinhuang, K., Jun, W., Hong, W., Ilhan, A.A., Jun, L., Yuehe, L., 2009. Biosens. Bioelectron. 25, 901–905.
Xu, C., Wang, X., Zhu, J.W., 2008. J. Phys. Chem. C 112, 19841–19845.
Yang, T., Li, Q., Li, X., Wang, X., Du, M., Jiao, K., 2013. Biosens. Bioelectron. 42, 415–418.